Supporting Information

Enhanced Photochemical Hydrogen Evolution From Fe_4S_4-Based Biomimetic Chalcogels Containing M^{2+} (M= Pt, Zn, Co, Ni, Sn) Centers

Yurina Shim[1], Ryan M. Young[1], Alexios P. Douvalis[2], Scott M. Dyar[1], Benjamin D. Yuhas[1], Thomas Bakas[2], Michael R. Wasielewski[1], Mercouri G. Kanatzidis[1,*]

1) Department of Chemistry and Argonne-Northwestern Solar Energy Research (ANSER) Center, Northwestern University, Evanston, Illinois 60208, United States

2) Department of Physics, University of Ioannina, 45110 Ioannina, Greece

* To whom correspondence should be addressed: m-kanatzidis@northwestern.edu

Experimental

Synthesis of starting materials:

$[(CH_3CH_2)_4N]_4Sn_4S_{10}$ was used as a source of $[Sn_4S_{10}]^{4-}$, and an adamantane tetrahedral cluster was synthesized by the procedure adapted from the literature.[1] In an evacuated three neck rounded bottom flask, 220 mg (2mmol) of K_2S, 475 mg (4mmol) of Sn, 257 mg (8mmol) of S, and 924 mg (6 mmol) of $(CH_3CH_2)_4NBr$ were reacted in ethylenediamine at 100˚C under N_2 for 12 hours, filtered, and washed with 50 mL of ethanol to yield a light gray powder of $[(CH_3CH_2)_4N]_4Sn_4S_{10}$ (yield ~70 %). The washed $[(CH_3CH_2)_4N]_4Sn_4S_{10}$ was dried in the vacuum oven overnight. The characterization by SEM/EDS and powder XRD were reported in previous publication.[2]

$(Ph_4P)_2[Fe_4S_4Cl_4]$ was used as a source of $[Fe_4S_4]^{2+}$ and the synthesis was performed in a nitrogen-filled glovebox following the established procedures.[3,4] 1.0 g of $FeCl_2$ (7.89 mmol), 1.56g of NaSPh (11.80 mmol), 1.48 g of Ph_4PCl (3.94 mmol), and 0.32 g of S (9.86 mmol) were dissolved in 40 mL of acetonitrile and stirred for 1.5 hr at room temperature. The brown solution was filtered, and 200 mL of ether was added to the filtrate. After settling overnight, the brown solution was filtered and washed with ether, yielding a black crystalline product. These black crystals were re-dissolved in acetonitrile to give dark brown solution and were filtered. To the dark brown filtrate, an excess amount of ether was added and allowed to stand ~48 hr. The resulting crystals were filtered, washed with ether, and allowed to dry under nitrogen to obtain black $(Ph_4P)_2[Fe_4S_4Cl_4]$ powder (~55%).

Third Metal Precursors: K_2PtCl_4, $Sn(OAc)_2$, $Co(OAc)_2$, $Ni(OAc)_2$ and $Zn(acac)_2$ were purchased from Aldrich and used as received.

Synthesis of Chalcogels (alcogels): Chalcogel synthesis was performed in a nitrogen-filled glovebox in a similar way as binary chalcogels. In typical synthesis, 0.2-0.25 mmol (~0.26g) of $[(CH_3CH_2)_4N]_4Sn_4S_{10}$ was dissolved in 5 mL of formamide (FM) with vigorous stirring to give white translucent solution. The solution became clear after being filtered. In a separate vial, 0.1 mmol (~0.12g) of $(Ph_4P)_2[Fe_4S_4Cl_4]$ was dissolved in 1 mL of *N,N*-dimethylformamide (DMF). The $(Ph_4P)_2[Fe_4S_4Cl_4]$ solution was then added dropwise to the $[(CH_3CH_2)_4N]_4Sn_4S_{10}$ solution while shaking manually after each drop over ~ 2 minutes. When the addition of $(Ph_4P)_2[Fe_4S_4Cl_4]$ is complete, a reflective black liquid results. This liquid is poured into a clean vial, covered, and left undisturbed at room temperature for ~5 min. Then the 0.2 mmol of desired third metal precursor was dissolved in 1mL FM. The solution was added dropwise to the reflective viscous black mixture of $[(CH_3CH_2)_4N]_4Sn_4S_{10}$ and $(Ph_4P)_2[Fe_4S_4Cl_4]$ with manual shaking after each drop. The entire viscous black liquid solidified into a rigid gel after ~ 2-7 days. When the rigid gels were formed, the gels were soaked in a 4:1 (v:v) mixture of ethanol and water (3x), followed by pure ethanol (3x) to remove byproducts and impurities. The solvent is exchanged every 24 hours over a week.

Supercritical Drying of wet gels. A supercritical fluid dryer, Tousimis Autosamdri 815B Series A, was used to remove the solvent from the fully cleaned alcogels. Slices of the alcogel were placed into the critical point dryer chamber inside of a custom-built metal basket. The chamber was cooled with liquid carbon dioxide to 5°C. Liquid CO_2 was introduced to exchange ethanol over 8 hr and fresh CO_2 was introduced into the chamber every 20-30 minutes over 6-8 hr in order to remove ethanol completely. The supercritical drying procedure was done at elevated temperature of 41°C, and pressure of 1400 psi for 4 minutes. The gaseous CO_2 was then slowly bled out of the chamber at 100-150 psi/min.

Nitrogen adsorption measurements. The surface area of the aerogels were measured by nitrogen adsorption. The aerogels were degassed at 75°C under vacuum overnight before analysis. Nitrogen adsorption/desorption isotherms were obtained using a Micromeritics ASAP 2020 instrument at 77K. The surface area was measured using the Brunauer-Emmett-Teller (BET) model using a series of relative pressures P/P_0 from 0.05 to 0.3.

Electron Microscopy and Elemental Analysis. The surface morphology of spongy aerogel was imaged by Scanning Electron Microscope (SEM) and the relative atomic composition of the chalcogels was determined with energy dispersive spectroscopy (EDS). SEM was performed on a Hitachi S-3400N-II instrument equipped with an EDS detector. The powdered samples (either xerogel or aerogel) were ground and placed on carbon tape. Transmission Electron Microscopy was performed on a JEOL 2100F instrument. The powdered gel samples were soniccated in ether, and the resulting suspension is dropcast onto a holey carbon TEM grid.

Mössbauer Spectroscopy. ^{57}Fe/ ^{119}Sn Mössbauer spectra were collected in transmission geometry, using constant acceleration spectrometers equipped with ^{57}Co(Rh)/^{119m}Sn($CaSnO_3$) sources kept at room temperature. The Mössbauer sample holders were prepared and sealed in strict glovebox conditions under N_2 atmosphere, and then transferred to liquid N_2 (Oxford) or closed loop He (ARS) Mössbauer cryostats, where the measurements were carried out in vacuum (10^{-3} – 10^{-6} Torr) conditions. Calibration of the spectrometers was done using metallic α-Fe at 300 K, and the isomer shift values are given relative to this standard for the ^{57}Fe spectra and relative to SnO_2 for the ^{119}Sn spectra. Fitting of the spectra was done using a recently developed Mössbauer spectroscopy fitting program.[5]

Cyclic Voltammetry. In a conventional three-electrode setup using Chi 900B Potentiostat, Pt wire and Ag/AgCl were used for the counter and reference electrodes respectively. A 0.1M

tetrabutylammonium hexafluorophosphate in acetonitrile flushed with N_2(g) was used as an electrolyte solution. The slices of wet alcogel were placed on the surface of the working electrode (glassy carbon electrode or platinum electrode) by packing them with a blade gently. The electrolyte was then introduced to the cell carefully so that the alcogels were stable on the surface of the electrode. Nitrogen gas was bubbled through the cell gently for 5 minutes prior to the measurement and over the surface of the electrolyte during the measurement. Voltammograms were obtained by sweeping reductively.

Chronocoulometry. Chronocoulograms (CCs) were obtained with the set up used for *Cyclic Voltammetry* with the applied potential of -1.0 V vs. Ag/AgCl.

Impedance Spectroscopy. Impedance spectra were obtained in solution with the *Cyclic Voltammetry* experimental setup. The constant DC potential was -1000 mV vs. Ag/AgCl, with an AC amplitude of 10 mV. The frequency range was 500 kHz to 0.05 Hz. The spectra were modeled with a simple RC equivalent circuit (SI, Figure S7) with a constant-phase element to extract the values of specific resistance and capacitance.

Dye Functionalization Experiments. Dye fuctionaliztion was performed in the manner of solvent exchange in a vial wrapped with aluminum foil in the N_2(g) filled glove box. Fully washed alcogel (sliced) samples were soaked in the 10 mM solution of tris(2,2′-bipyridyl)ruthenium(II) chloride hexahydrate (Ru-bpy) in ethanol. After overnight, the old solvent was extracted out and a fresh dye solution was introduced. This dye solvent exchange was performed three times, followed by washing the excess Ru-bpy "resting" on the surface/pores of the chalcogels with pure ethanol three times over 3 days.

Infrared Spectroscopy. The samples were prepared by grinding the xerogels with cesium iodide. Fourier-transform infrared spectroscopy (Nicolet 6700) was used.

Transient Absorption. Pieces of the dye-functionalized gels were sonicated into 1,2-dichlorobenzene, forming a thick, viscous suspension. These suspensions were deposited onto glass substrates by spincoating, resulting in thin films of the gels. The photophysics of the dye-functionalized gels were then examined by various timescale transient absorption spectroscopies. Nanosecond transient absorption experiments are achieved by exciting the samples with 7 ns, 1.8 mJ, 416 nm pulses using the frequency-tripled output of a Continuum Precision II 8000 Nd-YAG laser pumping a Continuum Panther OPO. The probe pulse, generated using a xenon flashlamp (EG&G Electro-Optics FX-200), and pump pulse are overlapped on the film with the pump being focused to a spot size slightly larger than the probe. Films were illuminated through the deposited gel in a "front face" configuration. Kinetic traces are observed from 440-800 nm every 5 nm using a 416 nm long-pass filter, a monochromator, and photomultiplier tube (Hamamatsu R928) with high voltage applied to only 4 dynodes. Kinetic traces are recorded with a LeCroy Wavesurfer 42Xs oscilloscope interfaced to a customized Labview program (Labview v. 8.6.1). Spectra are built from the single wavelength kinetic traces taken every 5 nm. Each kinetic trace is representative of an average of 200 shots over a five microsecond time window. To increase the signal to noise ratio of the spectral profiles, 5-10 ns segments of data are averaged together and the median time reported as the time of the spectral slice.

Femtosecond transient absorption experiments were performed using ~120 fs pulses derived from a commercial oscillator and regenerative amplifier (Spectra-Physics Tsunami/Spitfire), which produces a 1 kHz pulse train centered at 827 nm with 1 mJ/pulse. This output is immediately split by a 50% beamsplitter, yielding ~500 μJ/pulse for the transient absorption experiment. A small fraction (~5%) of this beam is further split and directed onto a computer-controlled translation stage to introduce the time delay between pump and probe pulses,

and then attenuated to ~1 μJ/pulse before focusing into a 3 mm sapphire plate, resulting in a fs continuum spanning 450-800 nm. The excitation ("pump") pulses are generated by second-harmonic generation in a lithium-triborate (LBO) crystal, yielding 120-150 μJ/pulse at 414 nm. Both pulses are then directed and focused into and overlapped in the sample. The pump beam is chopped before the sample at 25 Hz, and probe pulses are collected on a CCD array in a 20 pump-pulse-on / 20 pump-pulse-off pattern, and then differenced to yield the differential transient absorption spectrum at each given time delay. The overall temporal resolution of the system is ~120-200 fs across the detectable range, as measured by optical Kerr-gating cross correlation between the continuum probe and pump pulses.

Photochemical Hydrogen Evolution. In a nitrogen-filled glovebox, pieces of the dye-functionalized gels were transferred to a new scintillation vial. A solution of acetonitrile and water, 80:20 (v/v), containing 50 mM of lutidinium hydrochloride (proton source), 10 mM of sodium ascorbate (sacrificial electron donor), and 5mM of $Ru(bpy)_3Cl_2$ (excess Ru-bpy to prevent the displacement of Ru-bpy on the surface of the chalcogel by lutidinium) was added to the vial. After the vial was sealed and flushed with gaseous N_2 for 10-15 minutes, the vial was continuously illuminated with a 150 Watt Xe lamp (Oriel) with the total power of 100 mW/cm^2 to the sample. At specific time intervals, the headspace in the vial was sampled. After about 80 hr, the proton sources and sacrificial electron donors were recharged by extracting out the old solvent (2-3 mL) and injecting a fresh solvent (2-3 mL). The hydrogen was quantified with a gas chromatograph (Shimadzu GC-2014) equipped with a 5 Å molsieve column and a thermal conductivity detector using Argon as the carrier gas. Calibration was done with a 7% H_2/93% N_2 standard.

Tables

Table S1. Synthetic parameters and empirical formula for metal-free and M-ITS-cg3 chalcogels used in the work. The empirical formula of ternary chalcogels before and after functionalization with $Ru(bpy)_3Cl_2$ is calculated from the atomic % obtained from elemental analysis under EDS spectroscopy. Accurate empirical formula for the Sn linked ITS-cg3 could not be determined as the third metal shares the same element as Sn_4S_{10} building units. The [Fe](%) reflects the atomic percentage of Fe in the entire chalcogel. In order to show that $Ru(bpy)_3^{2+}$ is incorporated through ion-exchange, a detectable couter-cation, P from $(Ph_4P)^+$ and K from K_2PtCl_4, is included in the empirical formula in italic. P or K is not detectable after the functionalization.

Third metal	$[Fe_4S_4]$ (mmol)	M^{2+} (mmol)	Sn_4S_{10} (mmol)	[Fe] (%)	Observed Empirical Formula before functionalization	after functionalization
Pt	0.1	0.2	0.2	13	$K_{1.2}Pt_{2.8}[Fe_4S_4]_{2.2}[Sn_4S_{10}]_2$	$Ru_{3.4}Pt_{1.3}[Fe_4S_4]_{2.1}[Sn_4S_{10}]_2$
Zn	0.1	0.2	0.2	13	$P_{1.1}Zn_{1.3}[Fe_4S_4]_{2.0}[Sn_4S_{10}]_2$	$Ru_{3.1}Zn_{0.6}[Fe_4S_4]_{2.0}[Sn_4S_{10}]_2$
Sn	0.1	0.2	0.2	11	Not available	Not available
Ni	0.1	0.2	0.2	14	$P_{1.3}Ni_{0.7}[Fe_4S_4]_{2.8}[Sn_4S_{10}]_2$	$Ru_{1.7}Ni_{0.7}[Fe_4S_4]_{2.3}[Sn_4S_{10}]_2$
Co	0.1	0.2	0.2	8	$P_{0.6}Co_{1.7}[Fe_4S_4]_{1.4}[Sn_4S_{10}]_2$	$Ru_{1.6}Co_{1.1}[Fe_4S_4]_{1.2}[Sn_4S_{10}]_2$
None*	0.2	-	0.1	20	$P_{2.4}[Fe_4S_4]_{3.1}[Sn_4S_{10}]_2$	$Ru_{3.3}[Fe_4S_4]_{3.0}[Sn_4S_{10}]_2$

* None= Parent ITS-cg3: Fe_4S_4 - only containing chalcogel

Table S2. M-ITS-cg3 chalcogels' electrochemical parameters.

Third metal added	First reduction potential (mV)	Specific resistance (10^4 Ω)	Specific capacitance (10^5 F)
None*	-750	0.90 ± 0.33	4.12 ± 0.16
Pt	-500	27.5 ± 2.38	1.41 ± 0.02
Zn	-560	2.84 ± 0.01	4.30 ± 0.07
Co	-680	1.04 ± 0.02	6.90 ± 0.09
Ni	-700	2.18 ± 0.01	9.78 ± 0.10
Sn	-700	1.64 ± 0.05	3.00 ± 0.09

* None= Parent ITS-cg3: Fe_4S_4 - only containing chalcogel

Table S3. 57Fe Mössbauer parameters for parent and M-ITS-cg3 samples as resulting from the best fits of the corresponding spectra. Reported parameters for isolated analogous polycrystalline Fe_4S_4 complex, and native Fe_4S_4 bearing enzyme are listed for comparison.

Sample		^{57}Fe				
	T (K)	δ (mm/s)[1]	ΔE_Q (mm/s)	B_{hf} (T)	Area (%)	Assignment
ITS-cg3	77	0.45	1.21	-	50	Fe_4S_4 cluster
		0.47	0.72	-	50	Fe_4S_4 cluster
	10	0.45	1.21	-	4	Fe_4S_4 cluster
		0.47	0.72	-	4	Fe_4S_4 cluster
		0.45	-0.05	40.0	49	Fe_4S_4 cluster
		0.47	-0.09	14.8	43	Fe_4S_4 cluster
Pt-ITS-cg3	77	0.44	1.23	-	48	Fe_4S_4 cluster
		0.47	0.74	-	48	Fe_4S_4 cluster
		1.16	2.59	-	4	Fe^{2+} impurity
	10	0.46	1.24	-	18	Fe_4S_4 cluster
		0.48	0.75	-	18	Fe_4S_4 cluster
		1.18	2.90	-	3	Fe^{2+} impurity
		0.47	0.00	40.6	5	Fe_4S_4 cluster
		0.47	0.01	20.6	56	Fe_4S_4 cluster
Zn-ITS-cg3	77	0.43	1.22	-	50	Fe_4S_4 cluster
		0.44	0.75	-	50	Fe_4S_4 cluster
	10	0.45	1.22	-	1	Fe_4S_4 cluster
		0.44	0.75	-	1	Fe_4S_4 cluster
		0.45	-0.05	44.1	74	Fe_4S_4 cluster
		0.45	0.00	17.9	24	Fe_4S_4 cluster
Co-ITS-cg3	77	0.47	1.25	-	48	Fe_4S_4 cluster
		0.45	0.72	-	48	Fe_4S_4 cluster
		0.93	2.45	-	4	Fe^{2+} impurity
	10	0.48	1.26	-	32	Fe_4S_4 cluster
		0.47	0.73	-	31	Fe_4S_4 cluster
		0.96	2.45	-	4	Fe^{2+} impurity
		0.47	0.00	40.5	14	Fe_4S_4 cluster
		0.47	0.00	18.9	19	Fe_4S_4 cluster
Ni-ITS-cg3	77	0.46	1.16	-	47	Fe_4S_4 cluster
		0.43	0.72	-	47	Fe_4S_4 cluster
		1.15	2.55	-	6	Fe^{2+} impurity
	10	0.47	1.17	-	14	Fe_4S_4 cluster
		0.45	0.73	-	14	Fe_4S_4 cluster
		1.18	2.87	-	3	Fe^{2+} impurity
		0.46	0.00	42.2	9	Fe_4S_4 cluster

		0.46	-0.01	31.0	60	Fe_4S_4 cluster
Sn-ITS-cg3	77	0.44	1.17	-	28	Fe_4S_4 cluster
		0.47	0.65	-	28	Fe_4S_4 cluster
		0.47	1.66	-	27	Fe_4S_4 cluster
		1.04	2.41	-	17	Fe^{2+} impurity
	10	0.45	1.18	-	14	Fe_4S_4 cluster
		0.47	0.66	-	14	Fe_4S_4 cluster
		0.48	1.62	-	21	Fe_4S_4 cluster
		1.06	2.47	-	11	Fe^{2+} impurity
		0.46	-0.01	27.4	32	Fe_4S_4 cluster
		0.46	0.00	39.2	8	Fe_4S_4 cluster
$(NBu_4)[Fe_4S_4(SR)_4]$ (Ref. 6)	100	0.45	1.11			
		0.45	0.85			
Ferredoxin from Clostridium pasteurianum (Ref. 7)	77	0.44	1.08			

[1]Relative to α-Fe at 300K.

Table S4. ^{119}Sn Mössbauer parameters for parent and M-ITS-cg3 samples as resulting from the best fits of the corresponding spectra collected at 80 K.

Sample	^{119}Sn			
	δ[1] (mm/s)[1]	ΔE_Q (mm/s)	Area (%)	Assignment
ITS-cg3	1.42	0.05	33	Sn_4S_{10} cluster component I[2]
	1.64	1.89	67	Sn_4S_{10} cluster component II[2]
Pt-ITS-cg3	1.32	0.44	32	Sn_4S_{10} cluster component I[2]
	1.61	1.82	68	Sn_4S_{10} cluster component II[2]
Zn-ITS-cg3	1.00	0.24	39	Sn_4S_{10} cluster component I[2]
	1.20	0.68	61	Sn_4S_{10} cluster component II[2]
Co-ITS-cg3	1.11	0.00	94	Sn_4S_{10} cluster component I[2]
	1.27	3.60	6	Sn_4S_{10} cluster component II[2]
Ni-ITS-cg3	1.04	0.07	89	Sn_4S_{10} cluster component I[2]
	1.20	2.93	11	Sn_4S_{10} cluster component II[2]
Sn-ITS-cg3	1.12	0.36	55	Sn_4S_{10} cluster component I[2]
	1.23	3.67	20	Sn_4S_{10} cluster component II[2]
	0.09	0.56	25	M-linking Sn^{4+} ions

[1] Relative to $BaSnO_3$ at 77 K.
[2] Reference (2)

Figures

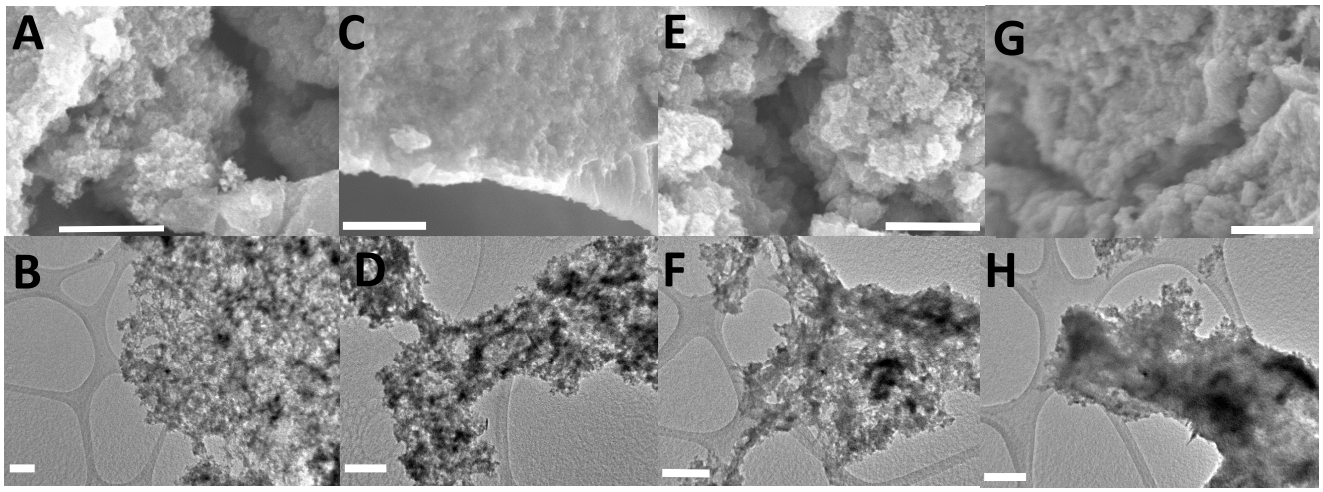

Figure S1. SEM and TEM images of M-ITS-cg3 samples. A,B) Pt-ITS-cg3 chalcogel; C,D) Zn-ITS-cg3 chalcogel; E,F) Ni-ITS-cg3 chalcogel; G,H) Sn-ITS-cg3 chalcogel. The scale bar in all SEMs is 10 μm; the scale bar in all TEMs is 200 nm.

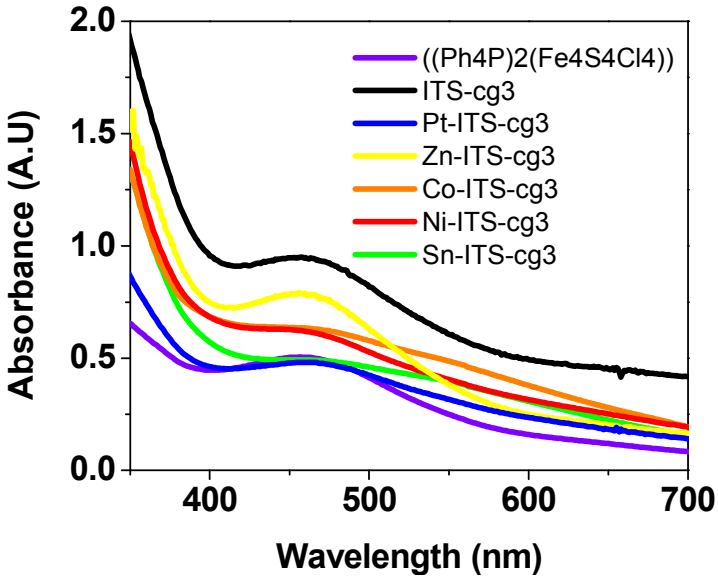

Figure S2. UV-vis spectra of chalcogel solutions after a thiol extrusion experiment, reflecting the absorption of the extruded $[Fe_4S_4(SPh_4)]^{2-}$ anion in parent ITS-cg3 and all M-ITS-cg3 chalcogels.

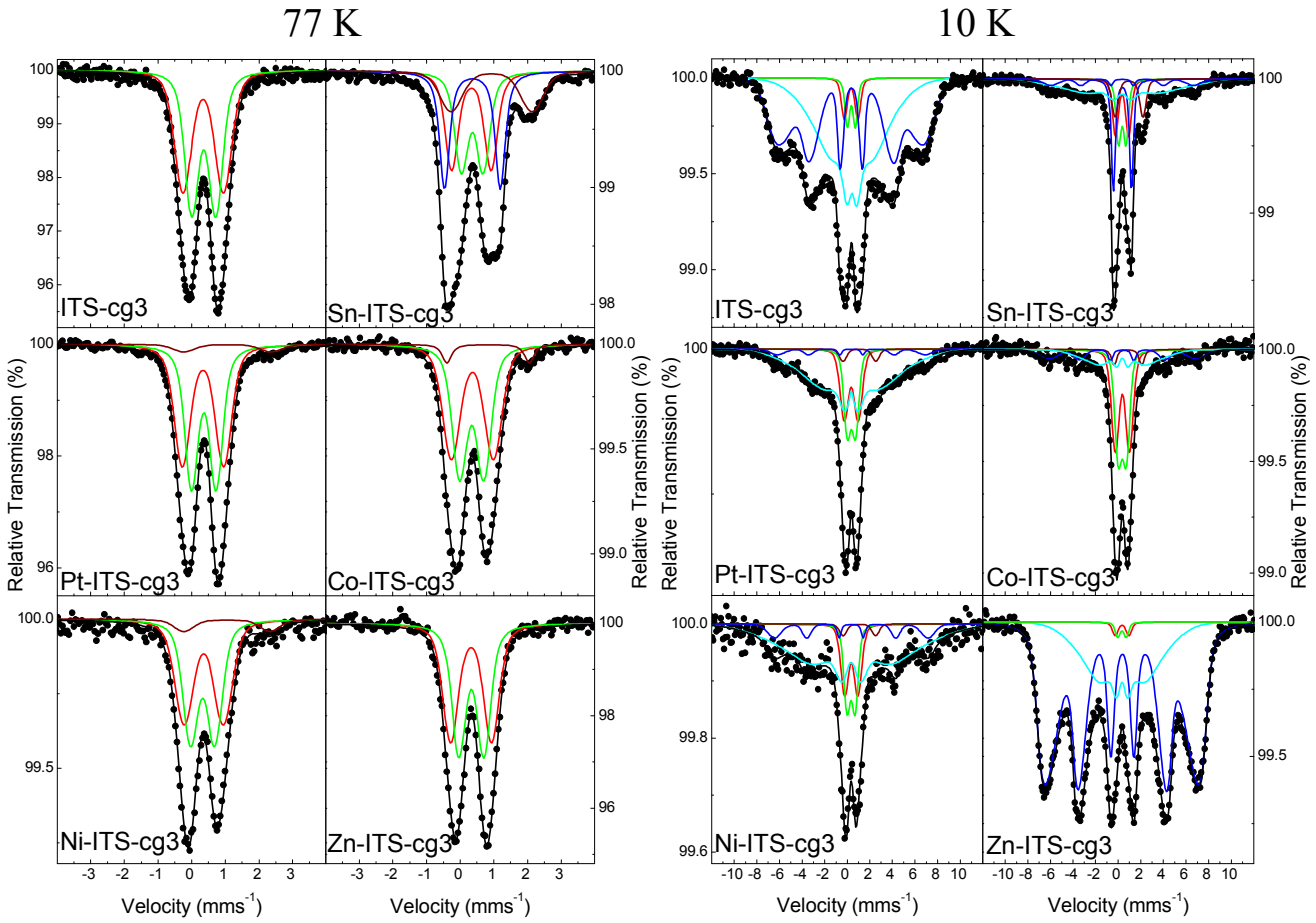

Figure S3. ^{57}Fe Mössbauer spectra of parent ITS-cg3 and M-ITS-cg3 samples recorded at 77 K and 10 K. Experimental data are denoted with points and their deconvolution with the relative components (colored continuous lines) is shown in each spectrum.

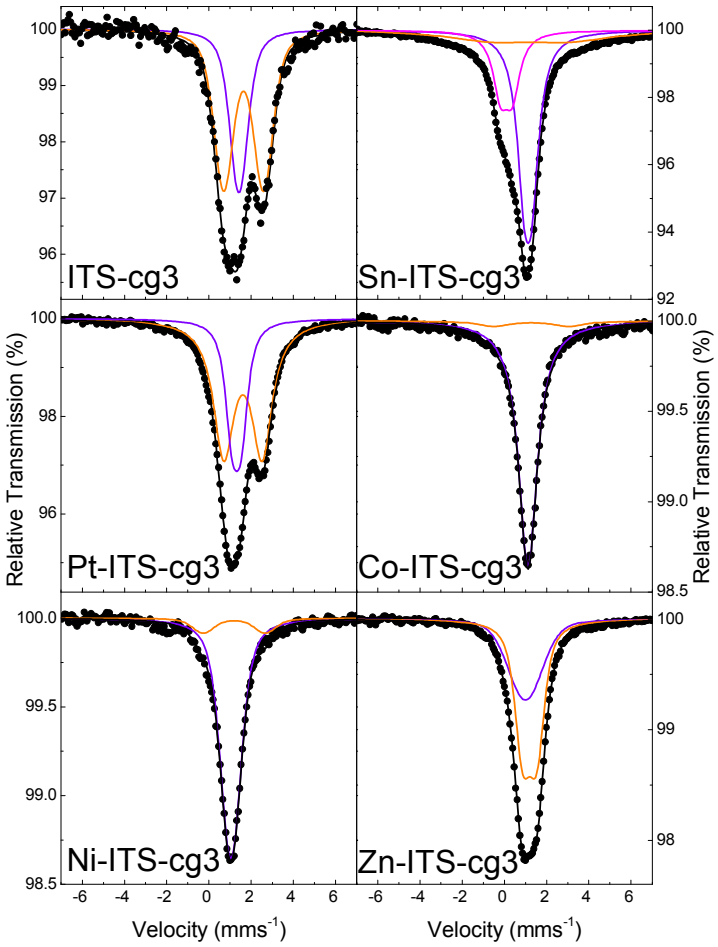

Figure S4. ^{119}Sn Mössbauer spectra of parent ITS-cg3 and M-ITS-cg3 samples recorded at 80 K. Experimental data are denoted with points and their deconvolution with the relative components (colored continuous lines) is shown in each spectrum.

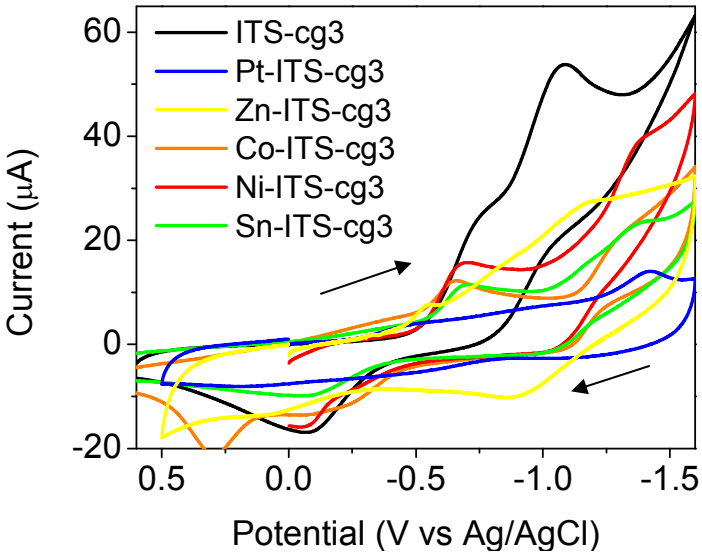

Figure S5. Full CVs of chalcogels scanned at a glassy carbon electrode in Bu_4NPF_6 + CH_3CN with a scan rate of 0.06 V/s.

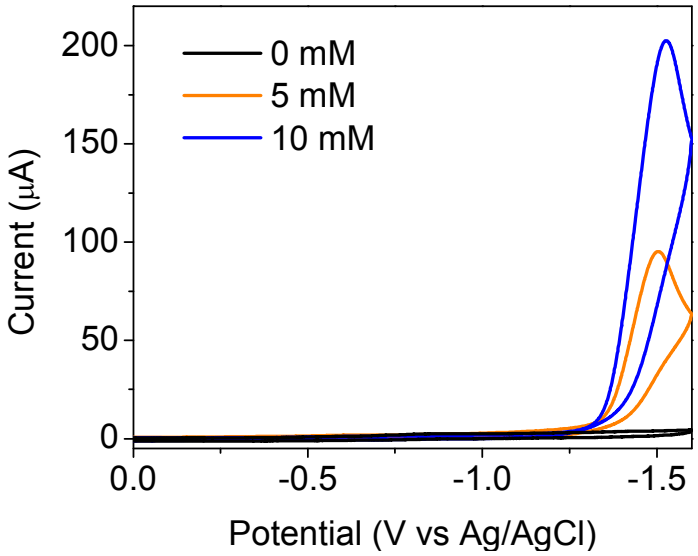

Figure S6. Full CVs of $[LutH]^+$ (0, 5, 10 mM) scanned at a glassy carbon electrode in Bu_4NPF_6 + CH_3CN with a scan rate of 0.06 V/s.

Calculation of active parts in biomimetic chalcogels

- The surface area of platinum working electrode (MF-2013 from BASi) is approximately 2.0 mm^2. ($\pi r^2 = \pi\ (0.8\ mm)^2 = 2.0\ mm^2$.)
- The average thickness of the gel deposited on the electrode is about 2.0 mm.
  --> Therefore, Gel volume = 4.0 mm^3 = 4.0× 10^{-3} cm^{-3}
- Skeletal density of the chalcogel obtained from the gas pycnometry is about 4.2 g/cm^3.

Therefore, in the chalcogel deposited on the electrode, there is about 9.7 ×10^{-6} mol of Fe_4S_4 clusters.

$$4.0 \times 10^{-3}\ \mathrm{cm^{-3}} \times \frac{4.2\ \mathrm{g}}{\mathrm{cm^3}} \times \frac{0.13\ \mathrm{g\ Fe}}{1\ \mathrm{g\ Gel}} \times \frac{1\ \mathrm{mol\ Fe}}{55.845\mathrm{g}} \times \frac{1\ \mathrm{mol\ [Fe4S4]}}{4\ \mathrm{mol\ Fe}} = 9.7 \times 10^{-6}\ \mathrm{mol\ [Fe4S4]}$$

If all [Fe_4S_4] clusters in the chalcogel deposited on the electrode participated in the one-electron reduction, approximately 0.94 C would be expected to pass through the chalcogel.

$$9.7 \times 10^{-6}\ \mathrm{mol\ [Fe4S4]} \times \frac{96458\ \mathrm{C}}{1\ \mathrm{mol}} = 0.94\ \mathrm{C}$$

From chronocoulometry data, the observed total charge passed after 10 sec in Co-ITS-cg3 is about 200 μC (Figure 5A) and it indicates that less than 1% of the Fe_4S_4 clusters in the chalcogel are electrochemically active within the 10 s timescale.

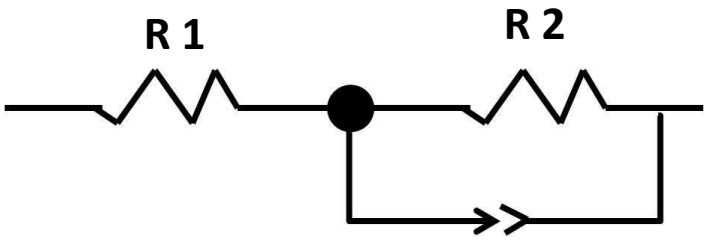

Figure S7. Equivalent Circuit Diagram used for fitting Impedance Spectra.

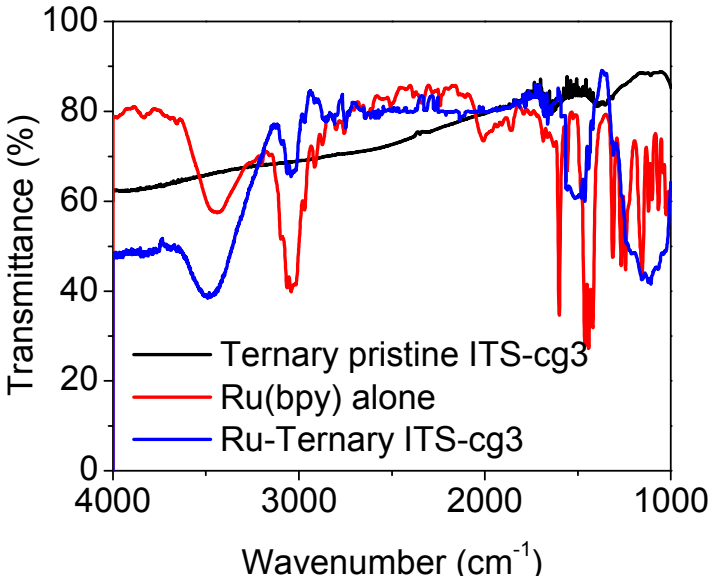

Figure S8. FTIR spectra of Pt-ITS-cg3 chalcogel functionalized with $Ru(bpy)_3^{2+}$ (Ru-Ternary ITS-cg3), unfunctionalized Pt-ITS-cg3 chalcogel (Ternary pristine ITS-cg3) and solid $[Ru(bpy)_3]Cl_2$ alone.

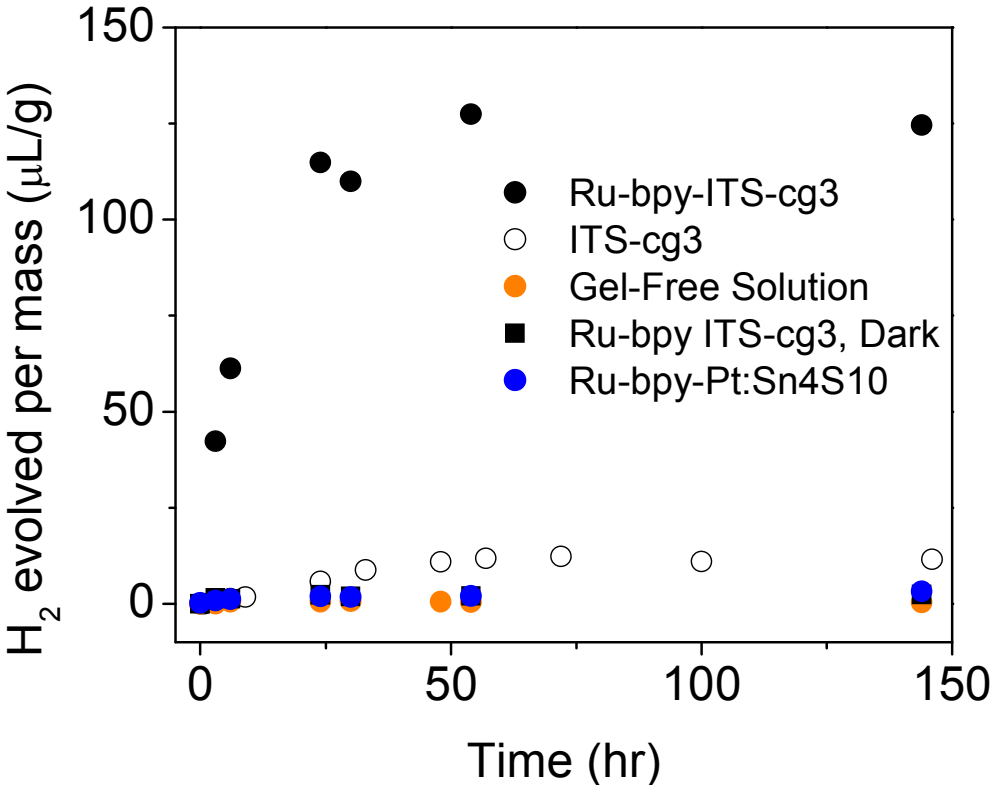

Figure S9. Light-driven H_2 production in the absence of $Ru(bpy)_3^{2+}$ (ITS-cg3), of ITS-cg3 (Gel-free solution), of light illumination (Ru-bpy ITS-cg3, dark), or of Fe_4S_4 clusters (Ru-bpy-Pt:Sn_4S_{10}) compared to the $Ru(bpy)_3^{2+}$ functionalized ITS-cg3. Pt:Sn_4S_{10} represents a chalcogel synthesized with Pt^{2+} and $[Sn_4S_{10}]^{4-}$. Absence of a light harvesting moiety, functionalized chalcogel, light source or Fe_4S_4 clusters all leads to negligible amounts of H_2.

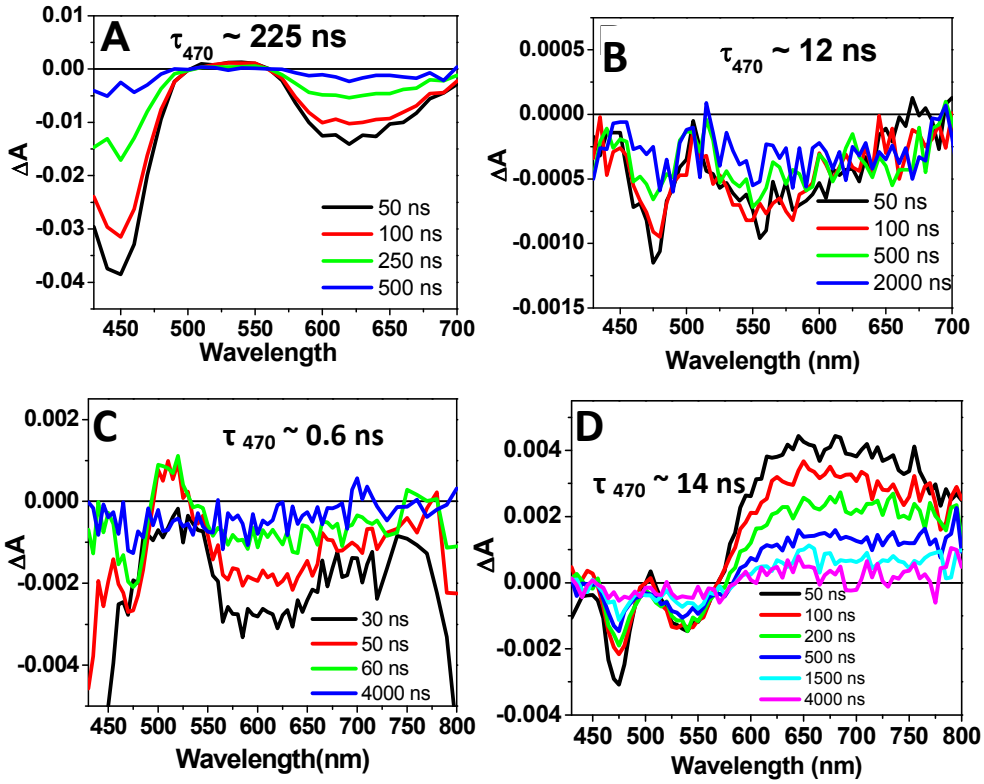

Figure S10. Nanosecond transient absorption spectra of (A) $Ru(bpy)_3^{2+}$ in solution, (B) ITS-cg3, (C) Pt-ITS-cg3, and (D) Co-ITS-cg3. The indicated lifetimes at 470nm are extracted from each series of spectra and reflect the lifetime of the ground state bleaching of $[Ru(bpy)_3]^{2+}$.

References

(1) Tsamourtzi, K.; Song, J. H.; Bakas, T.; Freeman, A. J.; Trikalitis, P. N.; Kanatzidis, M. G. *Inorg. Chem.* **2008**, *47*, 11920.

(2) Shim, Y.; Yuhas, B. D.; Dyar, S. M.; Smeigh, A. L.; Douvalis, A. P.; Wasielewski, M. R.; Kanatzidis, M. G. *J. Am. Chem. Soc.* **2013**, *135*, 2330.

(3) Coucouvanis, D.; Kanatzidis, M.; Simhon, E.; Baenziger, N. C. *J. Am. Chem. Soc.* **1982**, *104*, 1874.

(4) Wong, G. B.; Bobrik, M. A.; Holm, R. H. *Inorg. Chem.* **1978**, *17*, 578.

(5) Douvalis, A. P.; Polymeros, A.; Bakas, T. *J. Phys.: Conf.Ser.* **2010**, *217*, 0212014.

(6) Gray, H. B.; Malmstrom, B. G.; Williams, R. J. P. *J. Biol. Inorg. Chem.* **2000**, *5*, 551.

(7) Thompson, C. L.; Johnson, C. E.; Dickson, D. P. E.; Cammack, R.; Hall, D. O.; Weser, U.; Rao, K. K. *Biochem. J* **1974**, *139*, 97.